Photoproduction of Vector Mesons and Hyperons with a Beam of Linearly-Polarized Photons

Update of CLAS g8: E94-109, E98-109, E99-013, CAA2001-02

P.L. Cole[*†]
University of Texas at El Paso, El Paso, TX 79968

J.C. Sanabria[*]
Universidad de los Andes, A.A. 4976, Bogotá, Colombia

F.J. Klein,[*] H. Crannell, D.I. Sober
The Catholic University of America, Washington, DC 20064

J.D. Kellie,[*] **K. Livingston**,[*] D. Ireland, R.O. Owens, G. Rosner
University of Glasgow, G12 8QQ, United Kingdom

J.A. Mueller,[*] S.A. Dytman, S. Souren
University of Pittsburgh

D.J. Tedeschi,[*] M. Wood
University of South Carolina, Columbia, SC 29208

E. Pasyuk
Arizona State University, Tempe, AZ 85287

R. Schumacher, L. Todor
Carnegie Mellon University, Pittsburgh, PA 15213

H. Funsten
College of William and Mary, Williamsburg, VA 23185

S. Capstick
Florida State University, Tallahassee, FL 32306

C. Bennhold, B.L. Berman, W.J. Briscoe, K. Dhuga, I. Strakovsky
The George Washington University, Washington DC 20052

W. Roberts
Old Dominion University, Norfolk, VA 23529

J.-P. Didelez, M. Guidal, E. Hourany
Institut de Physique Nucléaire, Université de Paris, Orsay, France

J.-M. Laget
CEA-Saclay, DAPNIA/SPhN, Gif-sur-Yvette, France

Q. Zhao
University of Surrey GU2 7XH, United Kingdom

S. Boiarinov, V. Burkert, A.P. Freyberger, E.S. Smith
Thomas Jefferson National Accelerator Facility, Newport News, VA 23606

+

The CLAS Collaboration

∗ Co-Spokesperson on a g8 experiment
† Contact person

1 Introduction

The set of experiments forming the g8a run took place in the summer of 2001 (6/04/01 – 8/13/01) in Hall B of Jefferson Lab. These experiments [1, 2, 3, 4] made use of a beam of linearly-polarized photons produced through coherent bremsstrahlung, representing the first time such a probe has been employed at Jefferson Lab. Among the several new and upgraded Hall-B beamline devices commissioned prior to the production running of g8a were the photon tagger, the coherent bremsstrahlung facility (goniometer and instrumented collimator), a photon profiler, and the PrimEx dipole and pair spectrometer telescopes. We essentially commissioned a new beamline for photon running in Hall B. For the first phase of g8, i.e. g8a, we collected approximately 1.8 billion triggers in the photon energy range 1.75–2.2 GeV.

The scientific purpose of the g8 run is to improve the understanding of the underlying symmetry of the quark degrees of freedom in the nucleon, the nature of parity exchange between the incident photon and the target nucleon, and the mechanism of associated strangeness production. With the high-quality beam of the tagged and collimated linearly-polarized photons and the nearly complete angular coverage of the Hall-B spectrometer, we seek to extract polarization observables for the photoproduction of vector mesons and kaons at photon energies ranging between 1.1 and 2.2 GeV.

In this document, we shall first summarize the underlying motivations for our set of experiments.[1] We next will report on our results of the commissioning of the beamline devices and will recount the progress of our preliminary analysis of the g8a run. We then will argue that a continuation of g8 at lower energies is both necessary and timely. Because the second phase of g8 will gather data at lower energies, $1.1 < E_\gamma < 1.75$ GeV, ϕ production will be precluded.

2 Motivation for Using Linearly-Polarized Photons

The excitation spectrum of the nucleon is one of the most important constraints on any theory of strong interaction. The nonperturbative nature of QCD at low energies has represented a major challenge to hadronic physics, and has made necessary the use of phenomenological quark models. In these models, the internal structure of the nucleon is represented by three constituent valence quarks interacting with each other through a potential. An outstanding problem in our current day understanding of baryon spectroscopy is the question of the so-called "missing resonances". SU(6)⊗O(3) symmetric quark models predict far more resonances than have thus far been observed. One solution is to restrict the number of internal degrees of freedom by assuming that two quarks are bound in a di-quark pair [5], thereby lowering the level density of baryon resonances. An alternate solution has been put forward by Koniuk and Isgur [6] and others [7, 8, 9, 10, 11]. In these calculations it has been found that the missing resonances tend to couple weakly to the πN channel but stronger to the ρN, $\pi\Delta$, ωN, and $K\Lambda$ channels. Since most of our information on the baryon resonance spectrum comes from partial-wave analyses of $\pi N \to \pi N$, $\pi N \to \pi\pi N$, and $\gamma N \to \pi N$ measurements, these 'missing states' will clearly have escaped detection.

2.1 Photoproduction of Vector Mesons

Of special interest are those predicted resonances which are inconsistent with the di-quark model, like $P_{11}(1710)$, $P_{13}(1870)$, and $F_{15}(1955)$ which have – according to the quark model of Isgur and Karl [12] – a large branching ratio into ρN and ωN as well as reasonable photon-coupling. For this reason, a Hall-B electroproduction experiment [13] searches for resonances decaying via the

[1] For more information we refer the reader to the corresponding chapters in the proposals.

ωN channel, and one of the g1 photoproduction experiments [14] is a dedicated search for missing baryons that decay through the two-pion channel. We expect the identification of many of these resonances decaying through the ωN, ρN, or $\Delta\pi$ modes to be difficult due to their broad widths and narrow spacing. The sensitivity afforded by linearly-polarized photons will provide additional constraints in identifying these resonances, and such a measurement is complementary to experiments employing electron and unpolarized photons.

The quantities to be measured in our experiments with linearly-polarized photons are the spin density matrix elements of the vector meson [15]. With linearly-polarized photons, one has access to nine independent spin density matrix elements. Combinations of those correspond to the vector meson polarization,[2] the beam asymmetry Σ, the parity asymmetry P, and beam–vector meson double polarization observables. In the case of s-channel helicity conservation and natural-parity exchange ($J^\pi = 0^+, 2^+$), the decay angular distribution is given by $P_\gamma \sin^2\theta \cos 2\Psi$,[3] which corresponds to $\Sigma = P = 1$. In the case of unnatural-parity exchange ($J^\pi = 0^-$) the parity asymmetry is $P = -1$, – thus, linearly-polarized photons serve as a parity filter for t-channel processes.

By extracting these density matrix elements as functions of the Mandelstam variables, s and t, we shall obtain a *model-independent* pool of data. Being *bilinear combinations of the helicity amplitudes* , the density matrix elements form a meeting ground between experimentalists and theorists who predict the evolution of the helicity amplitudes through their models. A measurements of the evolution of these density matrix elements over a wide range of energies and four-momentum transfers squared will constrain the theory, and thereby give insight into the underlying production mechanisms.

The study of the ω production is of special interest since this vector meson is an isospin zero state and only couples to N^*, not to Δ^* states. The preliminary SAPHIR data on $\gamma p \to \omega p$ [17] as well as preliminary results of the CLAS electroproduction analysis show strong s-channel contributions around $W \simeq 1.9$ GeV. Moreover, due to its narrow width (Γ=8.4 MeV) it is – experimentally – comparatively simple to extract in missing mass distributions. In order to study the ρ photoproduction in the absence of a diffractive background, we also analyze the charge-exchange channel $\gamma p \to \rho^+ n$ where large contributions from resonant production are expected.

2.2 Photoproduction of Hyperons

A detailed study by Capstick and Roberts [18] on the decay of nucleon resonances into a strange baryon and a strange meson, suggests that some of the missing resonances may couple strongly to $K\Lambda$ and $K\Sigma$. Since $K\Lambda$ photoproduction can only involve isospin 1/2 resonances, one expects only a few of those states contributing to the s-channel for the reaction $\gamma p \to K^+\Lambda$. Therefore, the analysis required to identify the contributing N^* resonances should be simpler than for other channels.

The $\gamma p \to K^+\Lambda$ cross section data from SAPHIR [19], plotted in Fig. 1, show an enhancement at a center-of-mass energy of about 1.9 GeV. A calculation by Mart and Bennhold [20] finds a resonance with mass at 1895 MeV and interprets this structure as the result of the contribution of one of the "missing" resonances ($[D_{13}]_3(1960)$). More recently Saghai and collaborators [21, 22] have shown that the SAPHIR data can also be described by only taking into account the known N^* resonances and including off-shell effects and Λ^*-exchanges, as well as by quark model based calculations including all known N^* resonances. Both groups, however, point out that the presence of particular resonances in the s-channel have large effects on the beam asymmetry Σ, especially

[2] Via the decay into spin-0 particles, one has access to the tensor polarization components $T_0^2, T_{\pm 1}^2, T_2^2$. More information on these correlations in [16].

[3] Ψ is the angle between the direction of the photon polarization vector and the azimuthal of the decay plane.

the question of the claimed $D_{13}(1960)$ contribution cannot be settled without the measurement of the beam asymmetry and beam–recoil polarization observables.

The use of a linearly-polarized beam of photons, together with the measurement of the polarization of the recoil hyperon, gives access to the beam asymmetry Σ and the beam-recoil double polarization observables $O_{x'}, O_{y'}$, and $O_{z'}$. This data plus the data already taken with unpolarized and circulary-polarized photon beams during the sf CLAS-g1 run period (E-89-004 [23]) will provide an almost complete description of the reactions and will facilitate a *model-independent* partial wave analysis to identify intermediate resonances.

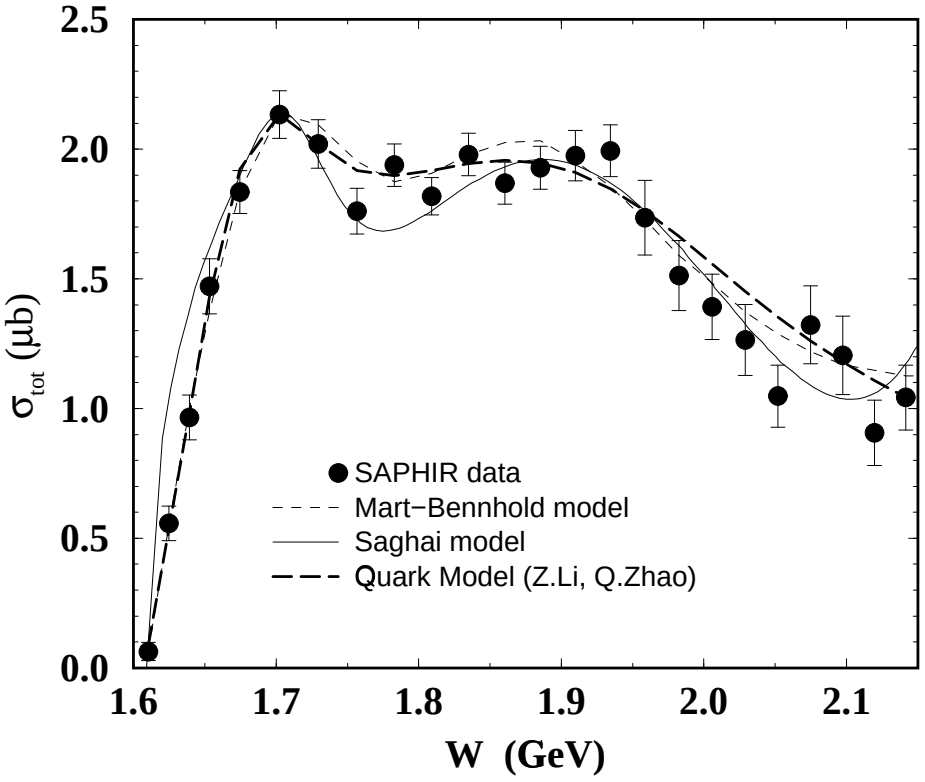

Figure 1: Total cross section for $\gamma p \to K^+\Lambda$ from SAPHIR in comparison with recent model predictions. The dashed line shows the prediction of the Mart–Bennhold model [20] which includes the "missing" $[D_{13}]_3(1960)$ resonance; the full curve represents a fit by Saghai [22] which only includes known N^* and Λ^* exchanges as well as off-shell effects; the dashed bold faced curve shows the result from quark model calculations.

3 Linearly-Polarized Photons via Coherent Bremsstrahlung

The technique of obtaining linearly polarized photons has been successfully employed at SLAC [24] and Mainz [25]. Detailed discussions of the underlying theory of coherent bremsstrahlung can be found in Refs. [26, 27, 28, 29, 30]. The g8 series of experiments with linearly polarized photons relies on the Hall-B coherent bremsstrahlung facility which was commissioned at the beginning of the g8a run period. Figure 2 shows a schematic diagram of the facility and a brief description of the main components follows.

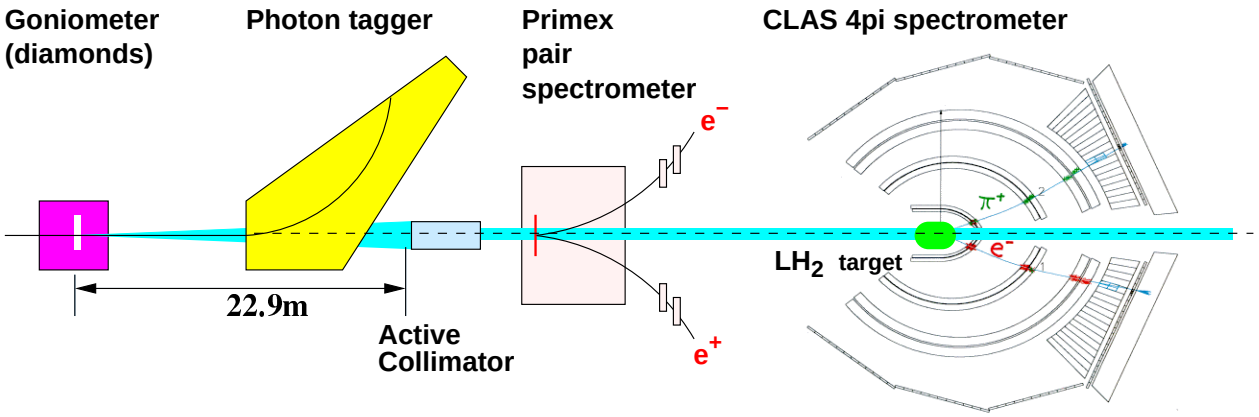

Figure 2: Layout of the components of the coherent bremsstrahlung facility in Hall-B

Diamond radiators

To obtain a high degree of linear polarization it is essential to have a diamond radiator which is thin ($< 100\mu$m) and has a very low mosaic spread (i.e. almost a perfect monocrystal). Several techniques have been developed by the Glasgow group for selecting crystals, including examination with a petrographic microscope and measurement of rocking curves at a synchrotron light facility. The rocking curve measures the width of the Bragg peak, and gives a very good indication of the quality of the diamond. Figure 3 shows the result of these measurements made on a 100μm synthetic crystal. The fact that the width of the Bragg peak is close to the theoretical value indicates that the crystal has a very low mosaic spread. On the basis of this, the crystal was ground down to less than 20μm. This was mounted on the radiator ladder with 2 *spare* crystals of 50μ and 100μ which were also selected on the basis of rocking curve measurements.

Goniometer

A goniometer with 6 degrees of freedom (3 rotation axes, 2 translation axes and a radiator ladder) was provided and installed by the group from GWU [31]. This can hold up to 6 radiators and is capable of orienting the diamond crystal to a precision of better than 10μrad.

Tagging spectrometer

The focal plane of tagging spectrometer has 384 plastic scintillators (E-counters) which provide signals to scalers and TDCs [32]. A major upgrade of the focal plane took place prior to running, since a high quality, low-noise photon spectrum is essential to determine the degree of linear polarization.

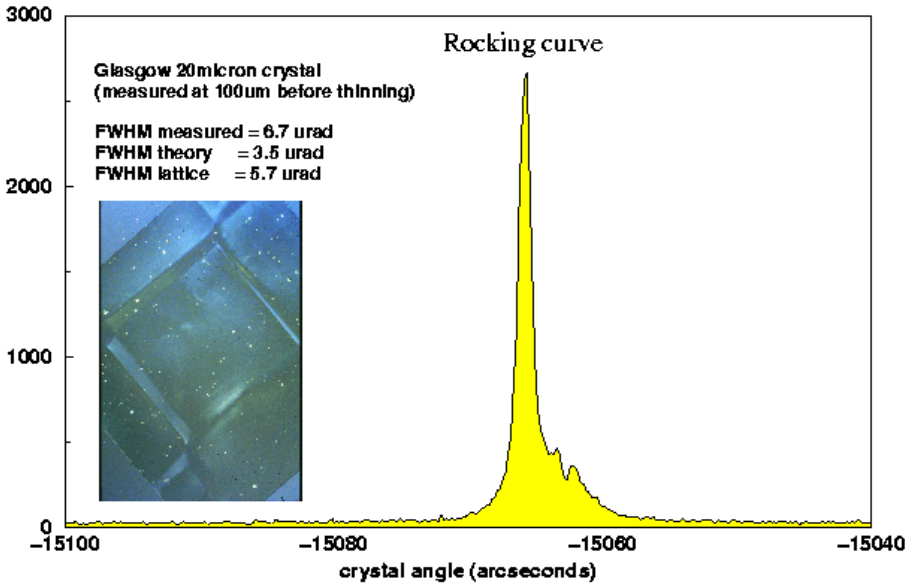

Figure 3: Measurements made on the crystal

This is described in more detail in a later section. The spectrum derived from the scalers gives rapid feedback on the uncollimated photon spectrum while the spectrum derived from the TDC (started by a downstream detector) shows the photon spectrum beyond the collimator.

Collimator

The polar emission angle of the coherent bremsstrahlung photon is correlated with its energy. Hence, tight collimation of the photon beam can improve the ratio of the coherent to incoherent component in the photon spectrum and increase the degree of linear polarization. An instrumented collimator of aperture 2mm was installed in the Hall B beamline at a distance of 22.9m from the radiator. The device was designed and tested by UTEP [33, 34] and engineered and built by the Institut de Physique Nucléaire in Orsay, France.

Coherent bremsstrahlung calculations

Selection of parameters such as collimation angle, crystal thickness etc. were made on the basis of analytic bremsstrahlung calculations using a variety of computer codes. A sample is shown in Fig. 4. As can be seen on the lower plot, with the 2mm collimator and the 20μm radiator it should be possible to obtain a polarization of $> 80\%$. The main uncertainty in these calculations was the angular divergence of the Jlab electron beam. A factor of σ=0.0035mrad was used in both dimensions. As is discussed in the next section, this turned out to be rather optimistic.

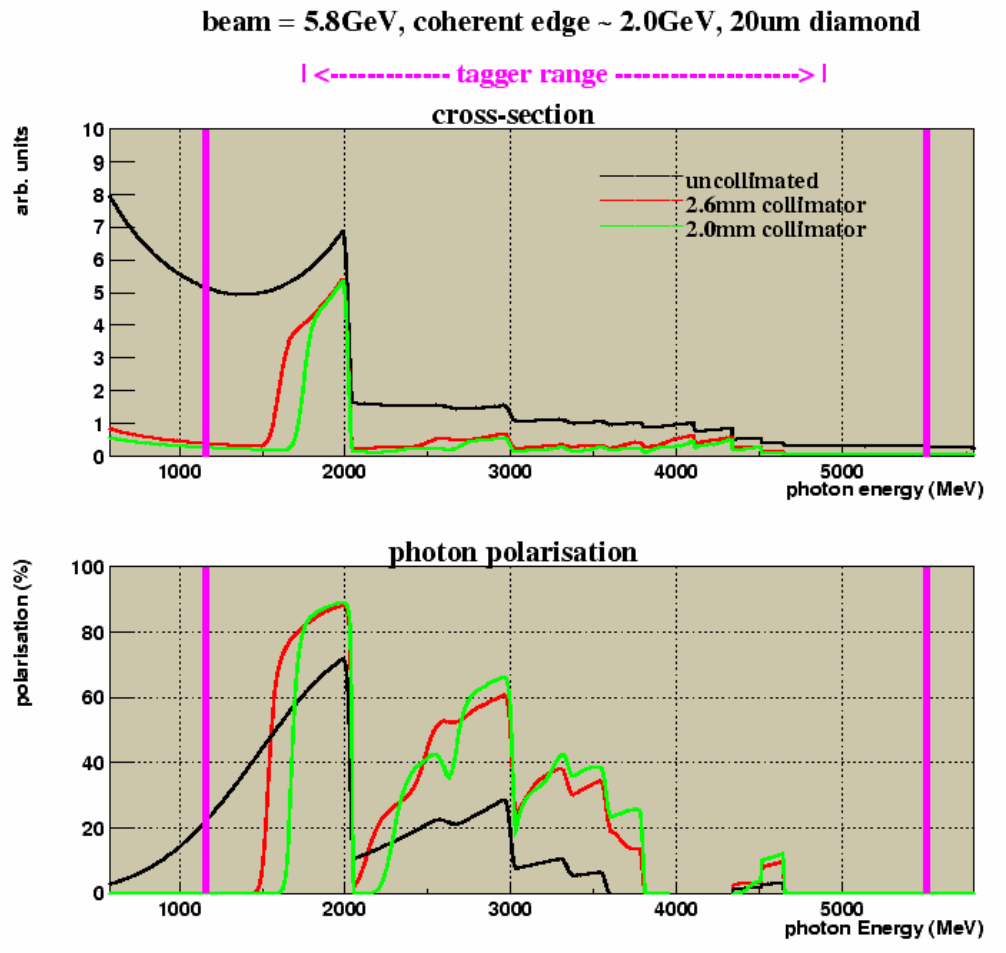

Figure 4: Coherent bremsstrahlung calcualtions made for a 20μm crystal and different collimatior sizes. These mare made using a modified version of the anb code [35].

4 Status of g8a

4.1 Linearly polarized photon production

To produce polarized photons of 2 GeV from a 6 GeV electron beam it is neccssary to have an angle of approximately 1μrad between the beam and the crystal lattice. Hence, a major part of setting up a cohent bremsstrahlung facility is the initial alignment of the crystal, where its default orientation relative to the beam is measured. The process used at Jlab is an extension of that developed by Lohman et al. [36], where a series of scans are taken. A scan consists of a sequence of small angular movements of the crystal and the corresponding accumulation of a photon energy spectrum. The alignment was done using a series of *quasi azimuthal* scans, where series of sinusoidal steps in horizontal and vertical rotation axes are used to set the [100] crystal axis at 60mrad from its

default position and sweep it though a 360° cone on the azimuthal axis. Figure 5 shows a simulated scan which illustrates the measurement of the angular offsets, together with the final scan obtained during the alignment procedure.

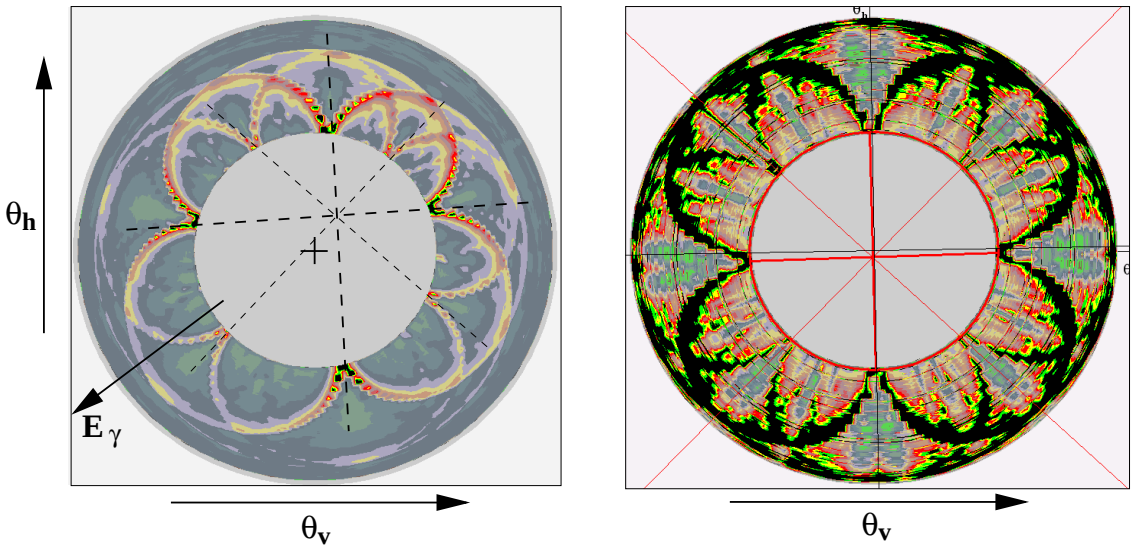

Figure 5: Left: Simulated scan illustrating the alignment method by fitting a template. Right: Final scan taken during the alignment process, indicating that the crystal is aligned to the required degree of precision.

The ridges on these plots show the energy of the coherent peak changing as the angle between the beam and crystal changes. As can be seen in the left hand figure, the orientation of the beam relative to the crystal can be found by fitting a template (shown with dashed lines) consisting of 8 lines separated by 45°. These lines must coincide with the points at which the ridges touch the inner circle (corresponding to the lowest tagged photon energy). The offset, in θ_v, θ_h coordinates, between the center of the template and the center of the circle gives the angular offset between the beam and the default crystal position, and the angle of the template gives the default azimuthal orientation of the crystal. The final scan has close to perfect 4-fold symmetry, which shows that the crystal is well aligned with the beam. This was the first major success of the commissioning period since it is a stringent test of the crystal quality, the goniometer performance and the ability of the tagger to provide fast feedback on the position of the coherent peaks. With the crystal aligned to the precision shown in Fig. 5 it was possible to make calibrations of photon energy vs angle on the 2 rotation axes, and to subsequently position the crystal in any required orientation relative to the beam.

Most of the production running was carried out with the coherent peak at 2GeV. Figure 6 shows the normalized photon spectrum before and after the collimator, where *normalized* here means that the spectrum obtained using the diamond radiator is divided by a reference spectrum obtained with an amorphous carbon radiator and the baseline is set to 100. The uncollimated data was obtained from free running scalers read online during the run. The collimated spectrum is derived from TDC hit patterns and has the random background subtracted; this is a preliminary spectrum based on the first pass though data and a rough timing calibration. Both data sets are fitted using the anb code [35] with the same parameter set, the only difference being the inclusion of the 2mm

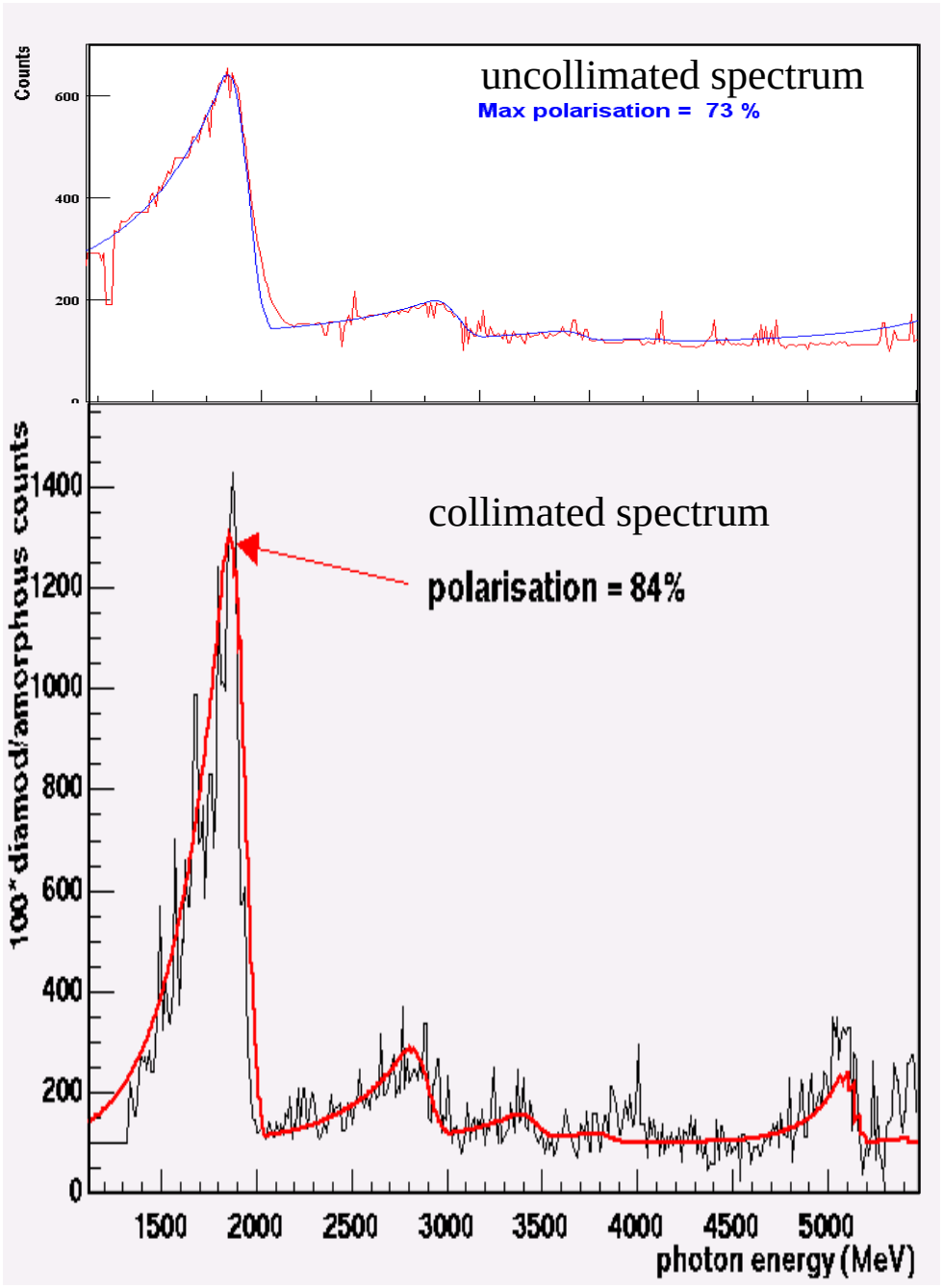

Figure 6: Normalized photon spectra before and after the collimator. Note, both plots are on the same vertical scale to highlight the enhancement due to the collimation of the photon beam.

diameter collimator for the bottom plot. The function parameters were adjusted until the agreement between calculation and data looked good to the eye. This will be done numerically as the analysis progresses. However, there is already very good agreement between the data and the calculation and on the basis of this evidence, we have succeeded in producing linearly polarized photons with a high degree of linear polarization (up to 84%).

Problems

- We were not able to use the 20μm crystal since the position of the coherent peak was very unstable and moved up and down the photon energy spectrum by up to 500MeV in a manner which we were unable to correlate (at least online) with any other effect. This was replaced by the 50μm crystal before production running.

- Although it was possible to fit the data with a bremsstrahlung calculation, the parameters differed from those used in the earlier simulations, even with a 50μm crystal (Fig. 4). In particular, the coherent edge in the data is much wider than was predicted before the experiment. To fit the edge it was neccessary to somehow increase the angular spread of the electron beam, either by increasing the crystal thickness (multiple scattering effect), or by adjusting the angular divergence parameters σ_x,σ_y. For the moment the fit has been achieved by assuming the crystal is 150μm, although it seems clear that it is the quality of the electron beam which is responsible (also see next item).

- The data shown are for the polarization plane in the vertical orientation (*perp*), i.e. where the angular spread of the beam in the vertical (or y) dimension has the dominant effect. The picture was much poorer for photons polarized in the horizontal plane (*para*), where the beam spread in the horizontal (or x) dimension is critical. In this orientation the edge was twice as broad as for the orthogonal orientation, and the peak height (i.e. the degree of polarization) much lower. No attempt has been made to quantify this yet. This was consistent with the harp scans which were take during the initial beam tuning and during running. The profile in the x dimension was always broader than that in y by at least a factor of 2. The aim is to get some consistent agreement between the σ_x,σ_y values required to fit the *para* and *perp* spectra, the beam position monitors and the harp scans. Based on the preliminary analysis of the polarized photon data so far, this seem to be an achievable goal.

4.2 Collimator

In addition to collimating the photon beam to enhance the degree of linear polarization, the collimator was designed with active components to provide feedback on the beam position with a sensitivity of at least 100μm. The collimator consists of a stack of 15mm-thick nickel disks with a 2mm hole at the center. A high proportion of showers produced in the first disk produces a signal in the four radially mounted scintillators which are sandwiched between the first and second disks. By comparing the asymmetries measured on line with the standard beam position monitors it was determined that the device was performing well beyond design specifications (cf. Fig. 7) and has the potential to be fed back to the beam steering in future experiments.

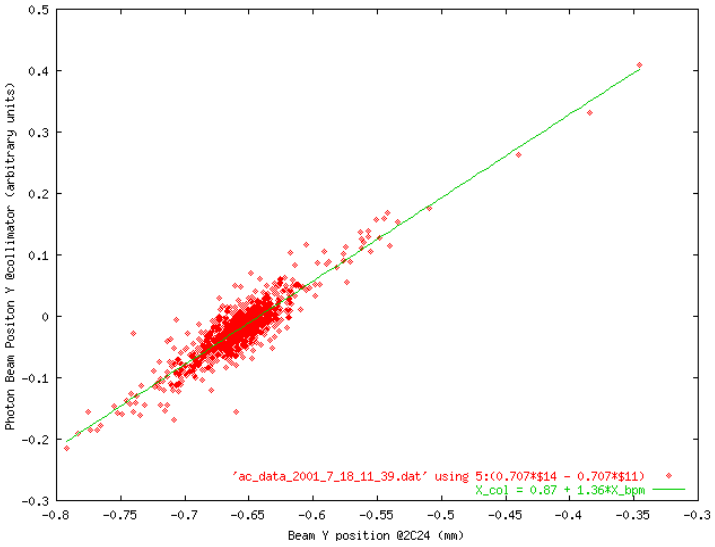

Figure 7: Correlation of the vertical beam position determined via the collimator scintillators and the beam y-position measured by the beam position monitor in front of the tagger magnet (2C24). Data from July 18, 2001.

4.3 PrimEx Dipole Magnet and Pair Spectrometers

We used the PrimEx dipole magnet in conjuction with two sets of pair spectrometers (PrimEx telescopes and CUA paddles) to monitor the collimated flux of photons. This system was also commissioned during the g8a run. While the background in the pair detectors was higher than anticipated, indicating a need for improved shielding, the system worked well, and provides an improved system over the old pair spectrometer which was located far down stream behind the CLAS target.

4.4 Startup Problems

We began commissioning with a newly upgraded tagger, a new thin diamond, and a new set of demands on the beam optics. All of these factors caused problems. The difficulties with the radiator were described in Section 4.1, the other problems are discussed here.

Tagger upgrade

The photon spectrum, as measured by the tagger, is the key diagnostic tool for aligning the reciprocal lattice vectors of the diamond radiator with respect to the incident electron beam to allow for coherent bremsstrahlung production. It is far from trivial to align the diamond radiator and it is absolutely imperative that the tagger be functioning well.

Priorto the beginning of the g8a run the tagger was upgraded with new E-counter PMT bases and new individual HV supplies for each E-counter. In addtion VME scalers were attached to each E-counter output. The previous scheme of ganging four E-counters to one HV channel did not allow for fine gain matching of the PMTs. The g8a run was the first experiment to make use of the tagger upgrade.

Unfortunately, due to a construction error, the new bases reduced the output from the PMT's by a factor of 5. The higher voltage required to overcome this problem caused excessive noise and prohibited obtaining clean spectra. For the first ten days of the g8a run we had scant beam, making it difficult to isolate the problems. In the middle of week two we discovered the photomultiplier base error. We stopped the run for four days to repair the error, after which the run proceeded much more smoothly. We are grateful to many members of the CLAS collaboration for pulling together in our time of need.

Beam instabilities

At times – and especially for the first four weeks – the beam was highly unstable, primarily in x. We had shifts on the order of 400 μm. Such instabilities compromised the data since the core of the coherent peak of the photon beam would be shifted from the central axis of the 2-mm hole of the instrumented collimator. The large number of beam trips will require us to remove up to 30% of the acquired triggers from the pool of data to be analyzed.

4.5 g8a Data and Calibrations

The g8a running period took place in the summer of 2001 (June 4 – August 13). The energy of the incident electron beam on the 50-μm thick diamond radiator was 5.7 GeV, with a nominal current of 7 nA. For our coherent bremsstrahlung data, we ran at two separate coherent peak edge energies: 2.07 GeV and 2.25 GeV. In the effort to study the systematics of the azimuthal dependence of the CLAS detector, we rotated the photon-beam polarization axis by 90° on several occasions. We did this by periodically rotating the diamond crystal between the Miller indices of $(02\bar{2})$ and (022) , so that these two mutually perpendicular reciprocal lattice vectors were properly aligned with respect to the incident 5.7 GeV electron. To further eliminate misleading or 'built-in' azimuthal dependences of the CLAS detector, we took several unpolarized-photon runs employing the amorphous 50-μm thick carbon radiator in lieu of the diamond crystal. These incoherent bremsstrahlung data will be our yardsticks for determining the polarization of the beam. These complementary data sets will aid us in understanding our azimuthal dependences and thereby will serve to reduce the systematic uncertainties in the differential cross sections of the hyperons and vector mesons.

Table 1: For the g8a production running period (12 July through 13 August 2001), we collected 1.85 billion triggers.

Coh. Peak (GeV)	Triggers (Million)
2.07	1400
2.25	350
unpolarized	100

4.5.1 Calibrations

Because of commissioning activities and tagger repairs, it was not until 12 July 2001 that we could commence production running. Between 12 July and 13 August 2001, we collected 1.85 billion triggers. Please refer to Table 1 for the details. Since the end of the g8a run on August 13 2001, we

have been working on the calibrations of the CLAS detector. As of the time of this writing, that is, for the past four months we have been performing calibrations on the following subsystems:

1. Accelerator-Radio-Frequency-Signal timing (RF).
2. Photon Tagger
3. Time of Flight hardware, timing, and energy loss
4. Start Counter
5. Drift Chamber

These calibrations are preliminary and it will not be until we have reconstructed a reasonable fraction ($\sim 10\%$) of the data that we will be able to assess, in detail, the quality of the calibrations, as well as the quality of the data. As of the time of this writing (3 Dec. 2001), we have been putting the final touches on the calibration of the Electromagnetic Calorimeters and we are about ready to start our first round of data reconstruction (i.e. 'pass 0 cooking'). We will reconstruct about 10% of the data for both monitoring the quality of the calibrations and to search any time dependencies. We expect that our newly installed monitoring devices will help us to filter out the off-axis photon beam events during periods of beam instabilities.

4.5.2 Rough reconstruction

In this subsection, we shall discuss a few 'online' plots of the g8a data. Soon we shall optimize our cuts with better calibrations. Granted the reconstructions are rather rough, but as indicated in Fig. 8, previous sets and online calibrations do serve to show the rough features. The upper left plot shows the photon energy spectrum on target, i.e. the tagged photon spectrum in coincidence with a charged track detected in CLAS which was consistent with a proton. For the missing mass distributions $MM_{pX}(\gamma p \to pX)$ in Fig. 8, we detect both the proton and π^+ and cut in the missing mass distribution $MM_{p\pi^+X}(\gamma p \to p\pi^+X)$ on the π^- peak. The upper right plot shows MM_{pX} over all 4-momentum transfer, t. The lower left plot is restricted to the forward region $|t| < 0.5$ GeV^2. Applying a simple cut in this missing mass spectrum ($0.60 < MM_{pX} < 0.95$ GeV) leads to the lower right panel, showing the $\cos\theta_{hel}$ distribution of the decay pion in the helicity frame for these events.

Figure 9 shows – for a smaller sample of events – the azimuthal modulation of the decay pion with respect to the polarization direction of the incident photon. The result was obtained for by subtracting the corresponding distribution for events at slightly higher photon energies than the coherent edge in order to eliminate the incoherent background. Since the CLAS acceptance varies drastically at forward angles, fiducial cuts were applied to cover the same azimuthal range. For s-channel helicity conservation, we expect the decay angular distribution to have a shape like $\sin^2\theta_{hel}\cos 2\Psi$ in case that the incident photon is 100% polarized. For unpolarized beam the distribution is flat in ϕ_{hel}. Our analyses are very, very preliminary; soon we shall optimize our cuts with better calibrations.

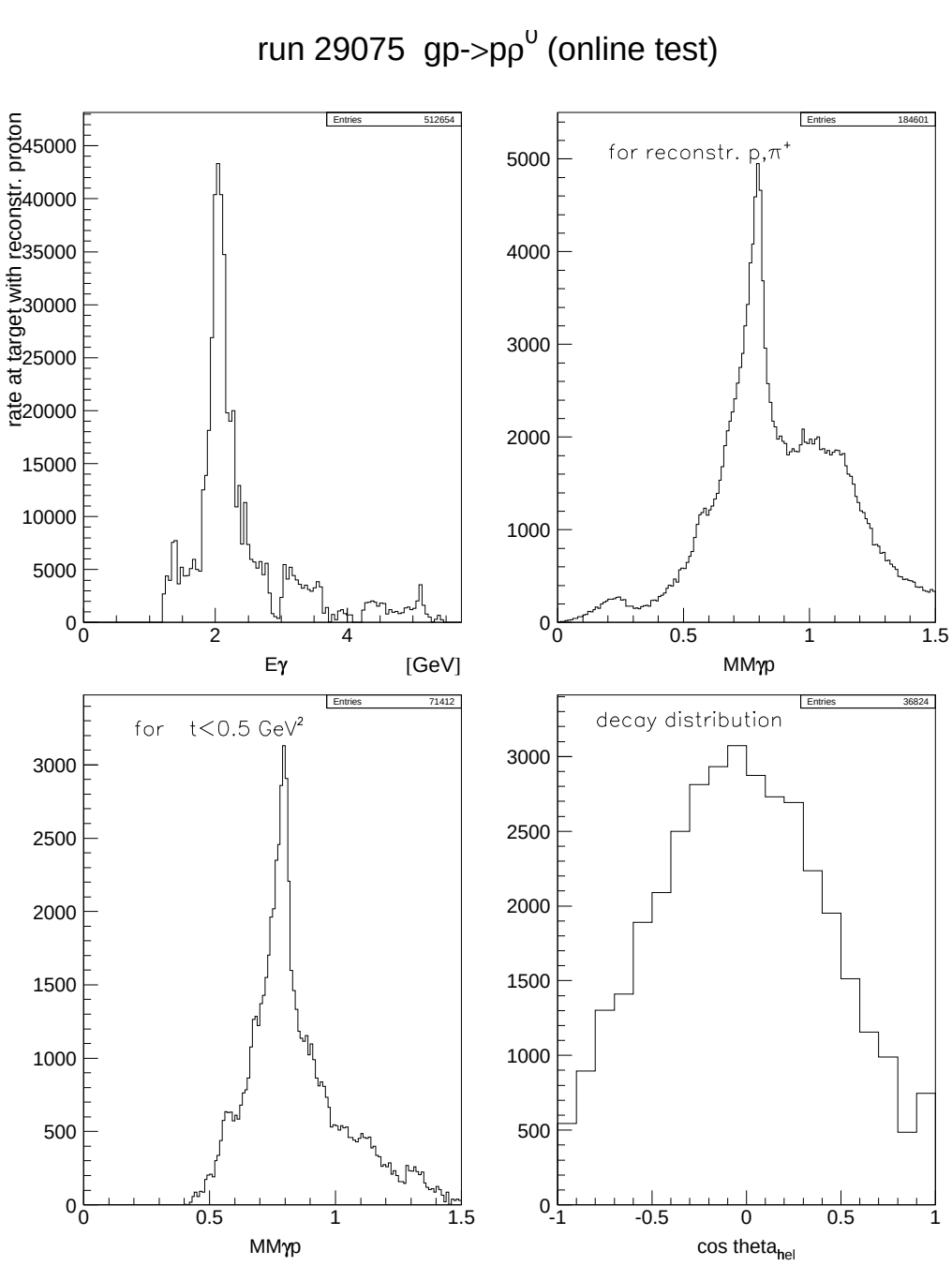

Figure 8: (Top Left) E_γ spectrum on the CLAS target for events with one proton detected in CLAS. (Top Right) Missing mass $MM_{pX}(\gamma p \to pX)$ for all $|t|$, (Lower Left) Missing mass $MM_{pX}(\gamma p \to pX)$ for $|t| < 0.5$ GeV^2, and (Lower Right) Pion $\cos\theta$ decay distribution in the helicity frame.

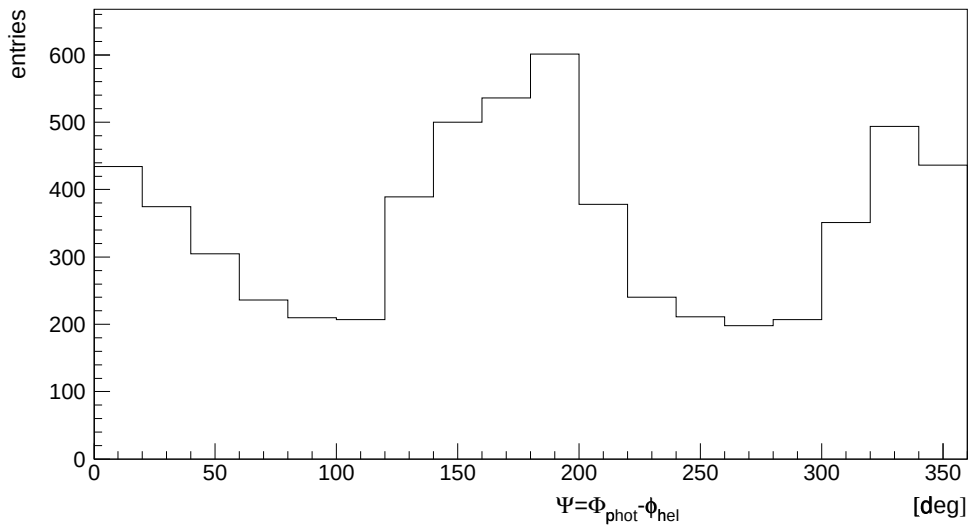

Figure 9: Azimuthal pion decay distribution with respect to the polarization direction of the incident photon.

4.6 Timeline for Cooking and Data Analysis

Before we may initiate the second phase of g8, we must first analyze the data of g8a. We anticipate to start the first pass of cooking of 10% of the g8a data by early February, 2002. The preliminary analysis from this data pool will allow us to monitor the stability and quality of the calibrations and will provide us a first chance to analyze and investigate the caliber of the data.

Below we list the tasks necessary for the data analysis and a rough timeline.

1. 15 January 2002 begin photon-flux normalization studies.
2. 15 March 2002 complete pass-0 cooking.
3. 15 March 2002 complete calibrations.
4. Nov. '01 – summer '03 Monte Carlo simulation studies of the acceptance of the CLAS detectors.
5. Feb. '02 – summer '03 analyze data
   (a) hyperons: Juan Carlos Sanabria (Bogotá, Colombia), James Kellie + Joseph Malone (Glasgow, UK).
   (b) rho mesons: Philip Cole (El Paso, TX), Ken Livingston + Chris Gordon (Glasgow, UK).
   (c) omega mesons: Franz Klein (Washington, DC)
   (d) phi mesons: David Tedeschi (Columbia, SC)
6. July '02 – Feb. '03 g8a cooking

We should be ready to publish our results by late summer 2003.

5 Goals of g8b

We seek to study the evolution of the spin density matrix elements as functions of the Mandelstam variables, s and t, in the effort to extract spin-parity information for the underlying baryon resonances which decay through the ρ or ω channel. The g8a data covers the photon energy range of 1.75 to 2.20 GeV. This gives a center of mass energy, $\sqrt{s}$, ranging from 2.04 to 2.24 GeV. To access the lower energy baryon resonances, we must, of course, reduce the energy of the incident photon. For example, in the Isgur-Karl model, the three-star rated P11(1710) decays primarily through the ρ channel. We will never see this resonance in the g8a data pool. Similarly, the one-star rated P13(1870) and not observed F15(1955) baryon resonances are predicted to decay mainly through the ω mode. These states are completely inconsistent with the di-quark model and it behooves us to search for them. Because the conjectured missing baryon resonances are broadly overlapping, we must study the density matrix elements over a wide range in c.m. energy in the effort to disentangle one resonance from another. So far we have covered only 180 MeV. We wish to extend our successful experiment to lower photon energies ranging from 1.1 to 1.75 GeV, which corresponds to 1.72 to 2.04 GeV in the center of mass. The second phase of g8 will extend the c.m. energy bite of the g8 data set by an additional and crucial 320 MeV.

In the case of the hyperon production, extending the measurements to the lower energy regime of g8b, coupled with those already obtained in g8a, will provide new data for the beam– and beam–recoil polarization observables (cf. Sec. 2.1) in the center-of-mass energies between 1.72 and 2.24 GeV. From Fig. 1 it is clear that we will span the energy region where both SAPHIR data and preliminary JLab data indicate various structures in the total cross section. The question of the claimed evidence for a $[D_{13}]_3(1960)$ resonance [20] can only be settled by means of making measurements of various polarization observables. The detailed mapping of these observables as a function of energy will constrain the partial wave analyses of the data and greatly facilitate extracting the individual contributions for each multipole in an almost model-independent way.

6 Requirements for g8b

Hall-B Beam Steering

We need better control of the electron beam at the goniometer position. Since the goniometer is located 16.7 m upstream of the nominal radiator position, the last group of steering magnets, located in front of the Hall-B tagger, cannot be energized for steering the beam. As it turned out during the g8a run, the current configuration of the Hall-B beamline is not completely achromatic. This means the parameters for the beam position cannot be kept sufficiently stable for optimal or successful operation of the goniometer. Due to this beam instability, a good portion ($\sim$ 30%) of the triggers taken during the g8a run will have to be filtered out. To improve control of the beam steering in the Hall-B extraction beamline, we require a new set of quadrupoles, which are to be placed in front of the goniometer This work will require some rearrangement of beamline components. This work is now scheduled for spring 2002.

Other Photon Beam Enhancements

A number of other projects are underway which will gradually improve the reliability of the polarized photon beam line. These are discussed briefly below.

1. Tagger Electronics.
   Currently, the tagger E-counter signals are fed into amplifier/discriminator boards. These

electronic modules have been an source crosstalk for large signals. Furthermore, the discriminated E-counter signals are output directly as free-running input into the scalers; this arrangement does not allow for the signals to be in placed in coincidence with other input signals. A redesign of the tagger E-counter electronics is in progress. The design will have two sets of scalers which can be independently gated. One of the E-counter signals will be put in coincidence with the corresponding T-counter; this logic should serve to reduce the background. Placing the other E-counter signal in coincidence with the pair spectrometer telescope, will provide information on the tagged photon rate downstream of the collimator.

2. Tagger E-Counters.
   In the winter/spring 2002, the PMT- and base-shielding of all counters are being redone. A system for moving a radiative source along the focal plane will be installed in the tagger. This source will allow for testing and preliminary gain matching of the tagger counters before the beam is available.

3. Tagger T-Counters.
   Currently, the maximum count rate per T-counter may not exceed 2 to 3 MHz without excessive dead time. This is because with the single hit TDCs used for the T-counters a random event, which occurs during the open gate before the real event, stops the TDC and causes the loss of teh necessary timing information. This effect can be greatly reduced by moving the correct event time much closer to the start of the TDC window. This technique will increase the acceptable rate per T-counter by at least a factor of two.

4. 20 μm diamond.
   The causes of major difficulties with the 20 μm diamond radiator which was used during the commissioning in June 2002 have to be investigated. Using such a thin diamond can be used during g8b will improve significantly the quality of the coherent bremsstrahlung beam.

5. Polarimeter.
   To determine the degree of linear polarization we have solely relied on theoretical calculation fit to the E-counter spectrum of the tagger. To assure accuracy of the results we need an independent means to measure the polarization of the photon beam. A pair polarimeter, constructed by NCCU and JLab, has been successfully tested in March, 2001 at the SPring8 facility in Japan. It will be ready for installation by the second phase of g8.

7 Beamtime Request and Timeline for g8b

We request to take data for g8b after the completion of the above mentioned improvements. **We expect to complete the second phase of g8 in 29 days**. Our request for this beamtime is set by the statistics needed for the ω channel. Data from Refs. [37, 17] indicate that the nondiffractive cross section at this photon energy resulting from the reaction $\gamma p \to \omega p$ is $d\sigma/dt \simeq 2.5$ μb/GeV^2 in the four-momentum transfer squared range of $0.4 < -t < 1.0$ GeV^2. The anticipated number of ω events produced per second within this t range can be calculated from the formula

$$\mathrm{N_{evts}} = \Phi N_{\mathrm{nucl}} \frac{d\sigma}{dt} \Delta t \simeq 5 \text{ events/sec},$$

Φ is the photon rate[4] which is taken to be 5×10^6 Hz, $N_{\rm nucl} = N_{\rm A}\rho\tau$, $\rho\tau$ is equal to (0.071 g/cm^3)(18 cm), and Δt has been set to 0.6 (GeV/c)^2.

We request to run at the energy setting of the electron beam between 4.2 and 4.5 GeV. The precise energy setting is to be determined upon the beam energy demands of the other experimental halls. We wish to run at a lower energy to minimize the beam trips and thereby minimize beam instability. In Table 2 we tabulate our beamtime request. We request to run for one day with the coherent edge set to 2.00 GeV to provide for overlap between g8b and g8a. This will allow for cross checking of the systematics. The remaining settings of the coherent peak will be unexplored territory.

Table 2: Beamtime request for the g8b run period

$(E_\gamma^{\rm coh.\ peak})$ GeV	$\sqrt{s}$ GeV	electron beam energy [GeV]	$x = E_\gamma/E_\circ$	Period hours
2.00	2.15	$4.2 < E_\circ < 4.5$	$0.44 < x < 0.48$	24
1.75	2.04	$4.2 < E_\circ < 4.5$	$0.39 < x < 0.42$	192
1.55	1.95	$4.2 < E_\circ < 4.5$	$0.34 < x < 0.37$	192
1.35	1.85	$4.2 < E_\circ < 4.5$	$0.30 < x < 0.32$	288

8 Summary

With the g8a run, we were able to show "proof of principle" that we can coherently produce a tagged and collimated beam of linearly-polarized photons from a 50 μm diamond radiator. The maximum degree of polarization exceeds 80%. For the first phase of g8, i.e. g8a, we collected approximately 1.8 billion triggers, which, after our data cuts and analysis, should give us well over 100 times the world's data set for ρs and ωs. From our experience with the g8a beamline and our recommendations for improvement, we expect to have a better quality beam of polarized photons with a high degree of linear polarization for the g8b run. In summary, a polarized photon beam represents a real enhancement of the JLab facility and its physics capabilities.

[4]We have assumed that the linearly polarized beam of photons has been collimated to two thirds of a characteristic angle.

References

[1] "Photoproduction of ρ Mesons from the Proton with Linearly Polarized Photons," Jefferson Lab E94-109, P.L. Cole, J.P. Connelly, and K. Livingston, cospokespersons.

[2] "Photoproduction of ϕ Mesons with Linearly Polarized Photons," Jefferson Lab E98-109, D.J. Tedeschi, P.L. Cole, and J.A. Mueller, cospokespersons.

[3] "Photoproduction of ω Mesons off Protons with Linearly Polarized Photons," Jefferson Lab E99-013, F.J. Klein and P.L. Cole, cospokespersons.

[4] "Photoproduction of Associated Strangeness using a Linearly Polarized Beam of Photons," CLAS Approved Analysis 2001-02, J.C. Sanabria, J. Kellie, and F.J. Klein, cospokespersons.

[5] D.B. Lichtenberg, Phys. Rev. 178 (1969) 2197;
R.E. Cutkosky and R.E. Hendrick, Phys. Rev. D 16 (1977) 2902.

[6] R. Koniuk and N. Isgur, Phys. Rev. D 21 (1980) 1868.

[7] S. Capstick and N. Isgur, Phys. Rev. D 34 (1986) 2809.

[8] S. Capstick, Phys. Rev. D 46 (1992) 1965;
S. Capstick, Phys. Rev. D 46 (1992) 2864.

[9] S. Capstick and W. Roberts, Phys. Rev. D 47 (1993) 1994;
S. Capstick and W. Roberts, Phys. Rev. D 49 (1994) 4570.

[10] S. Capstick and B.D. Keister, Phys. Rev. D 51 (1995) 3598.

[11] Z.P. Li, Phys. Rev. D 50 (1994) 5639;
Z.P. Li, Phys. Rev. D 52 (1995) 4961;
Z.P. Li, Phys. Rev. C 52 (1995) 1648;
Q. Zhao, Z.P. Li, and C. Bennhold, Phys. Rev. C 58 (1998) 2393;
Q. Zhao, Z.P. Li, and C. Bennhold, Phys. Lett. B 436 (1998) 42.

[12] N. Isgur and G. Karl, Phys. Lett. B 72 (1977) 109;
N. Isgur and G. Karl, Phys. Lett. B 74 (1978) 353;
N. Isgur and G. Karl, Phys. Rev. D 18 (1978) 4187;
N. Isgur and G. Karl, Phys. Rev. D 19 (1979) 4187.

[13] "Search for 'Missing' Resonances in the Electroproduction of omega Mesons", Jefferson Lab E91-024, H. Funsten, V. Burkert, M. Manley, B. Mecking, co-spokespersons.

[14] "A Search for Missing Baryons Formed in $\gamma p \to p\pi^+\pi^-$ using the CLAS and CEBAF," Jefferson Lab E93-033, J. Napolitano, spokesperson.

[15] K. Schilling, P. Seyboth, and G. Wolf, Nucl. Phys. B 15 (1970) 397;
D. Schildknecht and B. Schrempp-Otto, Nuovo Cim. 5A, (1971) 183.

[16] C.G. Fasani, F. Tabakin, and B. Saghai, Phys. Rev. C 46 (1992) 2430;
B. Saghai and F. Tabakin, Phys. Rev. C 53 (1996) 66;
M. Pichowsky, C. Savkli, and F. Tabakin, Phys. Rev. C 53 (1996) 593;
C. Savkli, F. Tabakin, and S.N. Yang, Phys. Rev. C 53 (1996) 1132;
B. Saghai and F. Tabakin, Phys. Rev. C 55 (1997) 917.

[17] F.J. Klein, Ph.D. thesis, Bonn-IR-96-008 (1996);
F.J. Klein, πN Newsletters, No. 14 (1998) 141.

[18] S. Capstick and W. Roberts, Phys. Rev. D 58 (1998) 074011.

[19] SAPHIR Collaboration: M.Q. Tran *et al.*, Phys. Lett. B 445 (1998) 20.

[20] T. Mart and C. Bennhold, Phys. Rev. C 61 (2000) 012201.

[21] W-T. Chiang, F. Tabakin, T-S. H. Lee, B. Saghai, Phys. Lett. B 517 (2001) 101.

[22] Z. Li, B. Saghai, Nucl. Phys. A 644 (1998) 345; Z. Li, B. Saghai, T. Ye, Q. Zhao, *work in progress.*

[23] "Electromagnetic Production of Hyperons", Jefferson Lab E89-004, R. Schumacher, spokesperson.

[24] W. Kaune *et al.*, Phys. Rev. D 11 (1975) 478.

[25] D. Lohman *et al.* Nucl. Inst. Meth. A 343 (1994) 494; J. Peise, M.S. Thesis, Universität Mainz (1989) ; D. Lohman, M.S. Thesis, Universität Mainz (1992); F. Rambo, M.S. Thesis, Universität Göttingen (1995); A. Schmidt, M.S. Thesis, Universität Mainz (1995).

[26] F.H. Dyson and H. Überall, Phys. Rev. 99 (1955) 604;
H. Überall, Phys. Rev. 103 (1956) 1055.

[27] H. Überall, Phys. Rev. 107 (1957) 223;
H. Überall, Z. Naturforsch. 17a (1962) 332.

[28] G. Diambrini-Palazzi, Rev. Modern Phys. 40 (1968) 611.

[29] U. Timm, Fortschr. Phys. 17 (1969) 765.

[30] R. Rambo *et al.* Phys. Rev. C 58 (1998) 489.

[31] NSF Major Research Instrumentation, NSF Award Number 9724489, W.J. Briscoe, K.S. Dhuga, and L.C. Maximon, co-PIs, The George Washington University, Washington, DC, 20052.

[32] D.Sober et al., Nucl. Inst. and Meth. A 440 (2000) 263.

[33] P.L. Cole, "The IPN-Orsay/UTEP Instrumented Collimator," August, 1999, 17pp. *unpublished.*

[34] A. Puga, Master's thesis, University of Texas at El Paso, "Calibration of the UTEP/Orsay Instrumented Collimator via the LabVIEW-Benchtop Data Acquisition System," December, 2001.

[35] A. Natter, *ANB Code*, URL `http://www.pit.physik.uni-tuebingen.de/~natter/software/brems-anb.html`

[36] D. Lohman, M Schumacher et al., Nucl. Inst. and Meth. A 343 (1994) 494.

[37] ABBHHM Collaboration, Nuovo Cim. 48 (1967) 262; Phys. Rev. 175 (1968) 1669.